Available online at www.eccomasproceedia.org
Eccomas Proceedia COMPDYN (2017) 1574-1589

ECCOMAS
Proceedia

COMPDYN 2017
6th ECCOMAS Thematic Conference on
Computational Methods in Structural Dynamics and Earthquake Engineering
M. Papadrakakis, M. Fragiadakis (eds.)
Rhodes Island, Greece, 15–17 June 2017

AN EMPIRICAL-BASED APPROACH FOR MODELING AND ASSESSMENT OF RC COLUMNS WITH PLAIN BARS

Gerardo M. Verderame[1] and Paolo Ricci[1]

[1] University of Naples Federico II, Department of Structures for Engineering and Architecture
Via Claudio 21 - 80125 - Naples - Italy
e-mail: {verderam,paolo.ricci}@unina.it

Keywords: reinforced concrete columns, assessment, plain bars, lumped plasticity, empirical-based, macromodel.

Abstract. *There is a growing need for numerical models simulating the non-linear behavior of Reinforced Concrete (RC) elements under seismic loads into inelastic range, and for capacity models assessing the deformation capacity of RC members, with emphasis on non-conforming existing buildings. As far as nonlinear modeling is concerned, several approaches have been proposed by different authors; among them, empirical-based macromodels for lumped plasticity modeling (e.g. Haselton et al., 2008) can represent an effective compromise between accuracy and simplicity. They have the great advantage of providing a complete characterization of the nonlinear response, accounting for all of the deformation mechanisms, and their reliability is based on the use of experimental data. They also allow evaluating error/dispersion measures of the simulated response compared to the experimental data they are based on, which can be suitably used for taking into account modeling uncertainties in seismic fragility analyses of RC frames. With regard to capacity models, different approaches have been proposed for the assessment of the deformation capacity of RC members, also for pre-normative purposes; in particular, as far as the seismic assessment of existing RC buildings is concerned, different capacity models have been developed for the ultimate deformation capacity of non-conforming elements subjected to different failure modes (e.g. Elwood and Moehle, 2005; Zhu et al., 2007).*

In this study, a nonlinear response macromodel is proposed for a specific type of member, i.e. RC columns with plain bars. To this end, a database of tests on RC columns with plain bars is collected from literature. The specimens have different axial load, material properties, geometry, and longitudinal and transverse reinforcement ratio. Force-displacement data are collected and processed for each specimen. The backbone of the experimental response is evaluated for each test, and predictive equations are developed for characteristics points, namely yielding, maximum strength, ultimate (conventional collapse) and zero resistance conditions, based on a statistical analysis of data.

doi: 10.7712/120117.5514.17488

1 INTRODUCTION

Current models for assessment and nonlinear modeling of RC elements are usually based on members with deformed bars (e.g. [1], [2], [3]). The post-elastic response of members with plain bars can be significantly different compared to members with deformed bars, due to the lower bond capacities [4][5] that, for instance, lead to higher deformability contribution of the fixed-end-rotation mechanism [6][7]. The objective of this paper is the derivation of empirical expressions providing the expected post-elastic response backbone for this kind of elements, through a regression analysis carried out on collected experimental data.

In literature, one of the most widespread empirical macromodels for predicting the nonlinear response of RC members has been proposed by Haselton et al. [8], which provide a trilinear response backbone and a parameter for modeling the stiffness/strength degradation, according to the cyclic response model proposed by Ibarra et al. [9]. The largest part of models for capacity assessment and modeling of RC members provides the prediction of the response already including the degradation due to cyclic displacement, as in the present study. Among these, the studies by Fardis and co-workers, which have proposed empirical-based formulations for chord rotation at yielding and "ultimate" (at 20% strength drop) [10][11][2], based on a large database of flexure-controlled experimental tests on RC elements. In the last years, several studies by Elwood and co-workers are focusing on the deformation capacity of existing non-ductile RC elements. Elwood and Moehle [12][13] proposed empirical formulations providing the drift at "collapse" (20% strength drop) and at "axial failure" (loss of vertical load-carrying capacity) of RC columns failing in shear following flexural yielding. These drift limits were used to model the shear-controlled response of RC elements (subjected to flexure-shear failure mode) in [14], by means of a modeling approach based on the use of the "limit state" material in OpenSees [15]. Aslani and Miranda [16] re-evaluated and simplified the formulations by Elwood and Moehle [12][13]. Zhu et al. [17] proposed a procedure for failure mode classification and, accordingly, empirical formulations for the prediction of drift capacity (at 20% strength drop) for columns failing in flexure or in shear/flexure-shear, and for the prediction of the drift capacity at axial failure of shear-controlled columns.

Different approaches have been adopted by international codes. The European standard EC8 adopted Fardis and co-workers' proposals, including correction coefficients for ultimate chord rotation of non-conforming elements [18][19], which account for their lower deformation capacity [20][2]. The US standard ASCE/SEI 41-13 [21] provides a procedure for the failure mode classification and, accordingly, empirical deformation capacity parameters calibrated to satisfy a target failure probability, depending on the failure mode. Such provisions were based on a proposal by Elwood et al. [1]. In [22] and [3] a modification to ASCE/SEI 41 provisions was proposed, in particular consisting of empirical expressions – not dependent on the expected failure mode – providing a median estimate of deformation capacity parameters.

A much lower amount of analytical studies regarding the assessment of the deformation capacity of RC members with plain bars is present in literature. The European standard EC8 provides specific expressions of the above-mentioned correction coefficients EC8 [18][19] for this kind of elements. These coefficients, in particular, account for the reduction of the ultimate chord rotation as a function of limited lap splice length. Different authors have evaluated the effectiveness of these coefficients, in some cases proposing improvements or alternative expressions [1][23][24]. Moreover, the effectiveness of current ASCE/SEI 41 provisions for elements with plain bars has been evaluated in [25], highlighting a significant conservatism.

In this study, an empirical macromodel is developed, providing the response envelope of flexure-controlled RC columns with plain bars. To this aim, a database of cyclic tests from literature is collected, and empirical formulations are proposed to evaluate the characteristic points of the response.

2 EXPERIMENTAL DATABASE

In this Section, the experimental database used for the empirical study reported in this paper is illustrated.

Cyclic experimental tests on ductile (flexure-controlled) RC columns with plain bars were collected. All the experimental responses were corrected accounting for P-Delta effects, if necessary, in order to be consistent with “Case I” reported in [26].

Table 1 reports the geometrical and mechanical characteristics of the 44 collected tests. 13 of them have overlapped longitudinal reinforcement, with a ratio between splice length and longitudinal bar diameter $15 \leq l_o/d_b \leq 47$.

The following parameters were extracted from the envelope of the experimental responses of the tests collected in the database. The obtained data are reported in **Table 2**.

- EI_{eff}: the effective stiffness was evaluated according to [27], i.e. as the stiffness secant to first yielding condition at theoretical first yielding moment, M_y; the ratio between EI_{eff} and the gross section stiffness, EI_g, was calculated (as the average between the two loading directions; if no cyclic displacement was imposed to the specimen prior to the attainment of the yielding condition, EI_{eff} was not calculated;
- M_{max}: the peak resistance was evaluated only if cyclic displacement was imposed to the specimen prior to the attainment of this condition; again, the average between the two loading directions was calculated;
- θ_{max}: if M_{max} was evaluated, chord rotation at peak resistance was considered, too;
- θ_{ult}: chord rotation at “ultimate” was evaluated corresponding to a 20% strength drop on the envelope of the response curve [10][13]; if $0.80 \cdot M_{max}$ was not reached in the softening response, the corresponding value was not reported; for this parameter, the lowest value between the two loading directions was considered;
- θ_0: chord rotation at zero resistance was evaluated extrapolating to zero the line interpolating the extreme envelope points of the softening branch of the response; again, the lowest value between the two loading directions was considered;
- K_0: softening stiffness toward zero resistance was identified with the slope of the above-described interpolating line used to evaluate θ_0.

An example application of the illustrated procedures is shown in **Figure 1**.

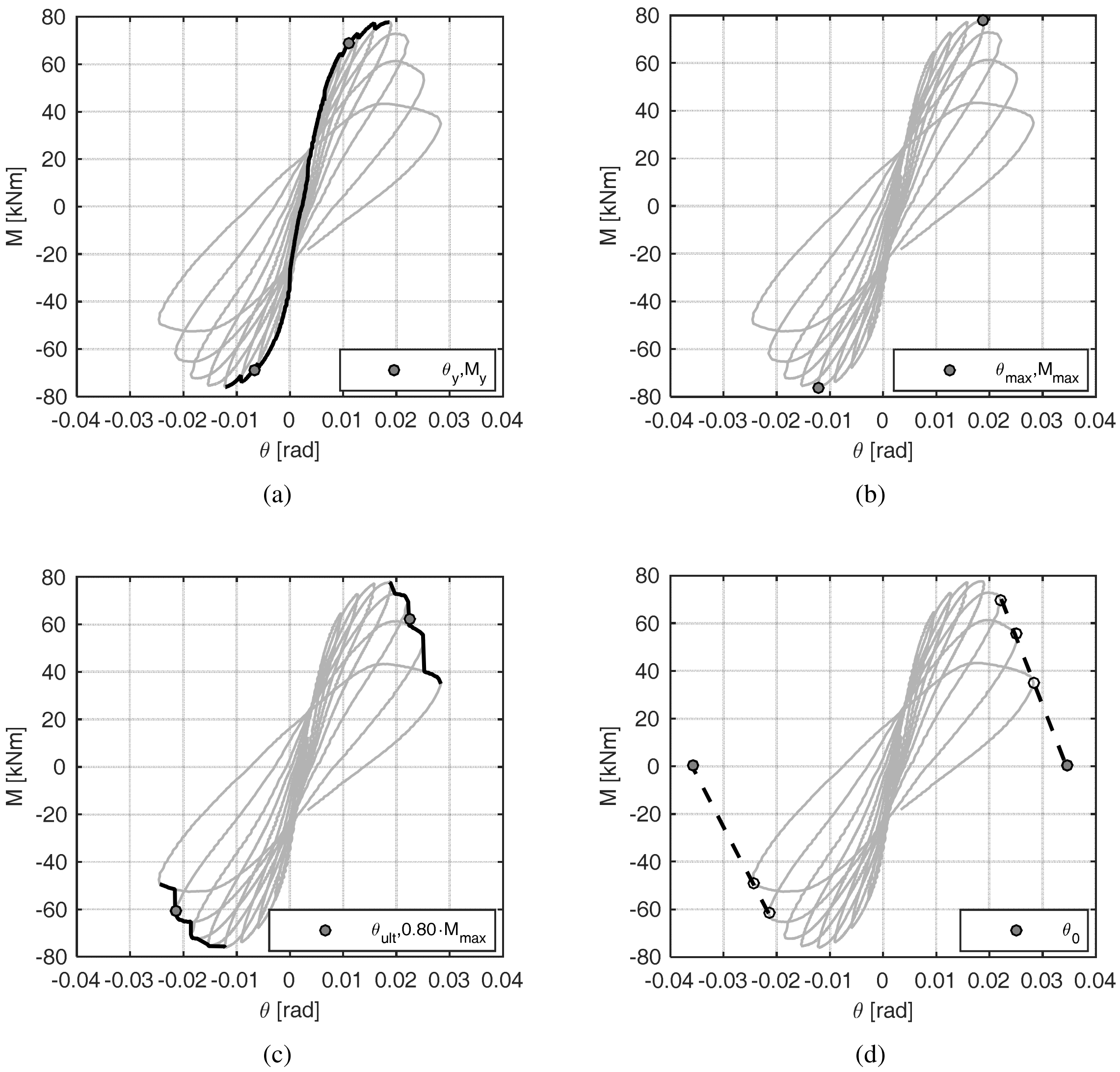

Figure 1: Example data extraction for Specimen Q-0L1 from [28] at yielding (a), peak resistance (b), "ultimate" (c), and zero resistance (d) conditions

#	Reference	Specimen	ν [-]	b [mm]	h [mm]	d [mm]	L_s [mm]	s [mm]	f_c [MPa]	f_y [MPa]	f_{yw} [MPa]	d_b [mm]	ρ_l [-]	ω_l [-]
1		C270-A1	0.12	300	300	270	1570	100	25	355	430	12	0.008	0.12
2		C270-A2	0.12	300	300	270	1570	100	25	355	430	12	0.008	0.12
3	[6]	C270-B1	0.12	300	300	270	1570	100	25	355	430	12	0.008	0.12
4		C540-A1	0.24	300	300	270	1570	100	25	355	430	12	0.008	0.12
5		C540-B1	0.24	300	300	270	1570	100	25	355	430	12	0.008	0.12
6		C540-B2	0.24	300	300	270	1570	100	25	355	430	12	0.008	0.12
7		S300P-c	0.20	300	300	270	1500	150	17.9	330	375	12	0.011	0.21
8	[29]	R300P-c	0.10	500	300	270	1500	150	19.2	330	375	12	0.010	0.17
9		R500P-c	0.10	300	500	470	1500	150	20.2	330	375	12	0.010	0.16
10	[30]	G5	0.20	300	300	270	1500	300	21.6	330	375	12	0.011	0.17
11		C-R30-s	0.20	500	300	270	1500	150	19.2	330	375	12	0.010	0.17
12		Q-0	0.44	250	250	210	1600	200	27	313	425	14	0.012	0.14
13		Q-0L1	0.41	250	250	220	1600	200	30.3	313	425	14	0.011	0.12
14	[28]	Q-0L2	0.42	250	250	220	1600	200	30.3	313	425	14	0.011	0.12
15		Q-0L1a	0.63	250	250	220	1600	200	28.1	313	425	14	0.011	0.12
16		Q-0L2a	0.57	250	250	220	1600	200	28.1	313	425	14	0.011	0.12
17	[31]	C	0.30	250	250	215	1600	200	25	372	351	14	0.011	0.17
18	[32]	Control	0.20	250	250	215	1600	200	25.6	372	351	14	0.011	0.17
19	[33]	C-O-1	0.47	200	300	265	1200	200	9.0	336	383	14	0.012	0.43
20		C3-S	0.14	300	300	270	1700	200	25.7	346	346	14	0.008	0.10
21	[34]	C16-S	0.40	300	300	270	1700	200	27.5	346	346	14	0.008	0.10
22		C18-S	0.40	300	300	270	1700	200	13.5	346	346	14	0.008	0.19
23	[35]	CC2N	0.20	200	200	185	750	100	23	356	356	10/6	0.012	0.18
24	[36]	WOS-C	0.15	250	250	220	750	200	22.9	370	370	12	0.008	0.13
25		HOS-C	0.15	250	250	220	750	200	24.8	370	370	12	0.008	0.12
26		S-L-0-00	0.40	350	350	302	2000	200	14	275	331	18	0.019	0.38
27	[37][38][39]	S-H-0-00	0.32	350	350	302	2000	200	20	284	331	22	0.029	0.41
28		R-NC-0-00	0.50	200	400	350	2000	200	12	275	331	18	0.029	0.67
29		1P2	0.21	350	350	315	2000	165	13.5	315	368	14	0.011	0.26
30		2P3	0.20	350	350	315	2000	165	12.2	315	368	14	0.011	0.29
31		3P3_N0.4	0.40	350	350	315	2000	165	13.1	315	368	14	0.011	0.27
32	[40][41][42]	4P4	0.20	350	350	315	2000	165	12.4	315	368	14	0.011	0.28
33		5P5	0.21	350	350	315	2000	165	11.4	315	368	14	0.011	0.31
34		6PV1	0.20	350	350	315	2000	165	12.5	315	368	14	0.011	0.28
35		7P3_U	0.20	350	350	315	2000	165	13.2	315	368	14	0.011	0.27
36		CPA-1	0.18	300	300	270	1700	200	21.2	405	410	12	0.008	0.16
37		CPA-3	0.18	300	300	270	1700	200	17.4	405	410	12	0.008	0.19
38		CPB	0.18	300	300	270	1700	200	20.3	405	410	12	0.008	0.17
39	[24]	CPC	0.18	300	300	270	1700	200	17.1	405	410	12	0.011	0.26
40		CPD	0.18	300	300	270	1700	200	18	405	410	12	0.011	0.25
41		CPE	0.18	300	400	370	1700	200	18	405	410	12	0.008	0.18
42		CPF	0.18	300	500	470	1700	200	18.3	405	410	12	0.008	0.18
43	[43]	S1	0.20	350	350	311	1425	265	29.5	325	350	20	0.023	0.25
44		S4	0.20	350	350	311	1425	265	25.9	325	350	20	0.023	0.29

Table 1: Database of cyclic tests on flexure-controlled RC columns with plain bars.

#	EI_{eff}/EI_g [-]	θ_{max} [rad]	M_{max} [kNm]	θ_{ult} [rad]	θ_0 [rad]	K_0 [kNm/rad]
1	0.34	0.015	66.3	0.062	0.260	272
2	0.38	0.020	68.4	0.058	0.237	303
3	0.38	0.013	63.2	0.063	0.147	602
4	0.38	0.018	98.9	0.037	0.132	933
5	0.42	0.017	96.4	0.038	0.142	810
6	0.48	0.013	101.5	0.032	0.111	1065
7	0.26	0.022	79.7	0.056	0.093	1712
8	0.21	0.026	100.9	0.068	0.127	1358
9	0.20	0.020	177.9	-	0.275	698
10	0.34	0.018	91.5	0.052	0.192	565
11	0.32	0.020	140.5	0.048	0.088	2736
12	0.55	0.015	72.4	0.019	0.030	6664
13	0.52	0.015	76.9	0.022	0.035	5657
14	0.78	0.011	83.5	0.013	0.021	14050
15	0.86	0.009	75.9	0.011	0.020	7238
16	0.87	0.011	83.0	0.013	0.021	13952
17	0.28	0.025	62.1	0.037	0.055	2752
18	0.20	0.040	53.2	0.060	0.080	2312
19	0.48	0.012	43.9	0.014	0.024	3432
20	0.34	0.025	88.1	0.035	0.059	3329
21	0.35	0.020	129.4	0.029	0.044	8723
22	0.37	0.018	71.4	0.031	0.085	1065
23	0.22	0.031	36.1	0.044	0.083	751
24	0.18	0.014	40.5	0.047	0.171	277
25	0.24	0.013	42.6	0.039	0.096	487
26	0.50	0.017	145.9	0.029	0.042	9916
27	0.48	0.022	191.1	0.040	0.063	7240
28	0.66	0.009	113.2	0.020	0.048	3145
29	-	0.028	102.6	-	0.301	351
30	-	0.028	95.6	-	0.149	797
31	-	-	-	0.030	0.062	2748
32	-	-	-	-	0.226	470
33	-	-	-	-	-	-
34	0.38	0.021	95.6	0.052	0.149	776
35	0.19	0.024	94.9	0.049	0.189	578
36	0.26	0.019	71.5	0.034	0.063	2024
37	0.32	0.024	65.4	0.045	0.081	1479
38	0.45	0.017	62.0	0.043	0.078	1447
39	0.23	0.025	83.6	0.048	0.072	2716
40	0.37	0.017	65.0	0.041	0.077	1447
41	0.15	0.028	118.8	0.041	0.057	6209
42	0.21	0.018	202.4	0.035	0.058	6325
43	0.24	0.016	192.6	0.024	0.049	6479
44	0.27	0.016	168.3	0.022	0.039	8435

Table 2: Extracted data at characteristic points of the base moment-chord rotation response envelopes (yielding, peak resistance, "ultimate", and zero resistance).

3 METHODOLOGY

The regression methodology adopted in this study consists of (i) the selection of potential predictive parameters, (ii) the analysis of the trends of the output (predicted) variable with the selected potential predictive parameters, (iii) the execution of regression analysis based on assumed functional forms, and (iv) the selection of the adopted formulation. This methodology is briefly illustrated as follows.

Based on previous literature studies and mechanical judgment, the following potential predictive parameters were selected: axial load ratio (ν); shear span-to-depth ratio (L_s/d); transverse reinforcement spacing-to-depth ratio (s/d); transverse reinforcement spacing-to-longitudinal bar diameter ratio (s/d_b); rebar buckling coefficient ($s_n=(s/d_b)\cdot(f_y/100)^{0.5}$) (already adopted by Haselton et al. [8]); geometrical (ρ_l) and mechanical (ω_l) longitudinal reinforcement ratio; geometrical (ρ_w) and mechanical (ω_w) transverse reinforcement ratio; compression-to-tension (including web) longitudinal reinforcement ratio (ω'/ω); concrete compressive strength (f_c); longitudinal steel yield strength (f_y); splice length-to-longitudinal bar diameter ratio (l_o/d_b). Furthermore, a "fixed-end-rotation coefficient", $(l_{ba}\cdot d_b)/(d\cdot f_c^{0.5})$, was tentatively used, trying to account for the influence of fixed-end-rotation on deformation capacity; this coefficient should be positively correlated with elements' deformability, since the expected rigid end rotation due to the slip of the longitudinal reinforcement from the anchorage should be positively correlated to the anchorage length (l_{ba}) and to the bar diameter (d_b), and negatively correlated to the square root of concrete compressive strength ($f_c^{0.5}$, correlated to the bond strength) and to section effective depth (d, correlated to the "rotation arm")

Then, the correlation between each output variable and the potential predictive parameters was analyzed through visual inspection and analysis of correlation coefficients. Parameters showing an unexpected (not mechanically explainable) correlation with the output variable were excluded.

Ordinary least squares regressions were carried out between each output variable (transformed in logarithmic form) and the input variables; these were assumed, alternatively, in their natural or logarithmic form, or not present (leading to *reduced* models, in the latter case). The *best* model was selected as the one characterized by the lowest Residual Sum of Squares (RSS) among all the *full* models.

Finally, F-tests were performed between the *best* model and all the *reduced* models searching for statistically significant differences. If the p-value was higher than a fixed significance level $\alpha = 0.10$ (assumed higher than 0.05 in order to reduce the risk of a "Type II" error [44]) the null hypothesis was not rejected, i.e. the reduced model was "accepted" as statistically equivalent to the best model. Among all the "accepted" reduced models, the one with the lowest number of predictive parameters and the highest p-value was selected. In some cases, a further parameter was included, if it led to a very significant increase in p-value. If possible, the expression was simplified in linear form. Statistics of the observed-to-predicted ratio (mean, median and Coefficient of Variation (CoV)) were calculated.

4 ANALYSIS OF RESULTS

The empirical formulations derived according to the above-described methodology are illustrated as follows for each parameter analyzed.

Effective stiffness

The regression obtained for EI_{eff}/EI_g includes the axial load ratio and the shear span-to-depth ratio, see **Eq. 1**. As expected, the effective stiffness increases with these parameters increasing. The strongest correlation is observed with the axial load ratio, consistent with previous literature and code expressions and mechanical-based judgment.

$$EI_{eff} / EI_g = 0.086 \cdot 7.6^{\nu} \cdot \left(1 + 0.23 \cdot L_s / d\right) \tag{1}$$

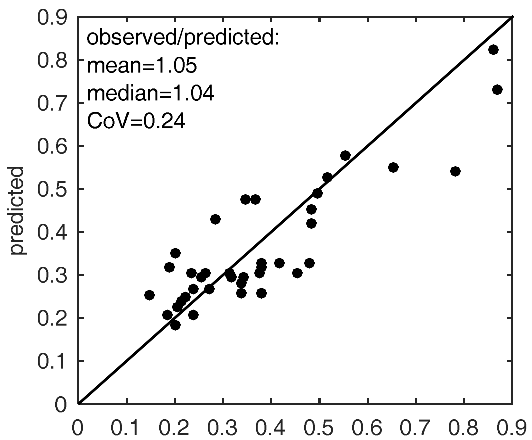

Figure 2: observed vs predicted EI_{eff} (Eq. 1)

Mean, median and CoV of the observed-to-predicted ratio are 1.05, 1.04 and 0.24, see **Figure 2**.

The observed values of EI_{eff}/EI_g can be compared with the ASCE/SEI 41-13 provisions; mean, median and CoV of the observed-to-predicted ratio are 0.82, 0.83 and 0.30, singularly equal to the values observed by Elwood and Eberhard [27] on rectangular columns with deformed bars; hence, the presence of plain bars does not seem to increase the deformability at yielding [11]. However, if a non-biased estimate of the expected stiffness has to be provided, the lower bound could be decreased from 0.30 to 0.20; mean, median and CoV of the observed-to-predicted equal to 0.98, 0.94 and 0.31 would be obtained, see **Figure 3**.

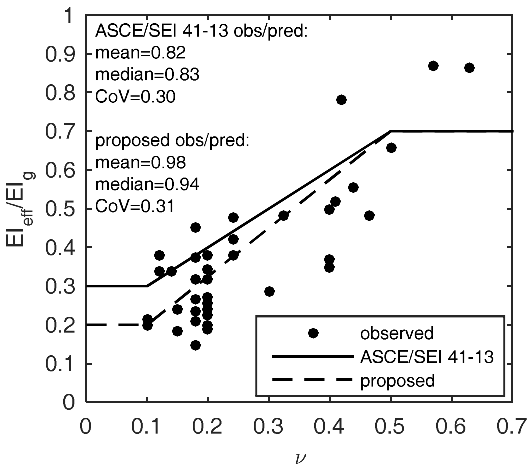

Figure 3: observed EI_{eff}/EI_g, ASCE/SEI 41-13 provision and proposed modification

Peak resistance

First, an attempt of predicting the observed flexural strength M_{max} through a section analysis is made, estimating the maximum expected moment as the moment calculated with a fiber analysis using a bilinear elastic-perfectly plastic model for the steel and the Mander et al. [45] constitutive relationship for the concrete, corresponding to a compressive strain of 0.004 in the extreme concrete fiber [27], M_{004}. Mean, median and CoV of the ratio between M_{max} and M_{004} are 1.08, 1.06 and 0.11, thus highlighting an experimental overstrength that has already been observed in literature, and can be explained through the confinement effect of the foundation element on the end section of the element [46]. Therefore, a regression analysis is carried out for the M_{max}/M_y ratio, but the obtained results do not show a significant scatter reduction compared to the observed values; thus, a simple mean value could be assumed for this ratio, i.e. $M_{max}/M_y = 1.17$.

Chord rotation at peak resistance

The regression obtained for θ_{max} includes the axial load ratio, the shear span-to-depth ratio and the splice length-to-longitudinal bar diameter ratio, see **Eq. 2**. Mean, median and CoV of the observed-to-predicted ratio are 1.00, 0.98 and 0.24, see **Figure 4**. A negative correlation is observed with the geometrical longitudinal reinforcement ratio, too, but it is not retained in the formulation selected according to the adopted methodology. Note the minimum between l_o/d_b and 50 was assumed in regression analysis.

$$\theta_{max} = 0.011 \cdot 0.21^{\nu} \cdot \left(1 + 0.29 \cdot L_s / d\right) \cdot \left(0.57 + 0.43 \cdot \min\left(l_o / d_b, 50\right) / 50\right) \tag{2}$$

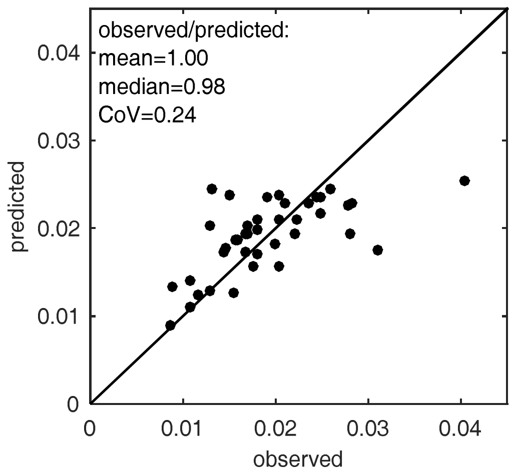

Figure 4: observed vs predicted θ_{max} (Eq. 2)

Chord rotation at "ultimate"

The regression obtained for θ_{ult} includes the axial load ratio, the mechanical transverse reinforcement ratio, the "fixed-end-rotation coefficient" proposed in this study, and the splice length-to-longitudinal bar diameter ratio, see **Eq. 3**. The terms related to the two latter coefficients could be approximated by linear expressions. Mean, median and CoV of the observed-to-predicted ratio are 1.02, 1.05 and 0.18, see **Figure 5a**. Again, the axial load ratio has the strongest influence also on this deformation capacity parameter. The beneficial effect of transverse reinforcement through the confinement effect on concrete in compression is demonstrated by the inclusion of the mechanical transverse reinforcement ratio. The inclusion of the "fixed-end-rotation coefficient" demonstrates the possibility of taking into account the higher deformability due to this deformation mechanism through the proposed coefficient. As for θ_{max}, the minimum value between l_o/d_b and 50 was assumed as predictive parameter. Note that, different from the usual approach based on correction coefficients [18][19], which are calibrated *a posteriori*, in this case a unique expression is derived for elements with continuous and lap-spliced longitudinal reinforcement.

Another regression analysis is performed excluding the "fixed-end-rotation coefficient", because in some situations the anchorage length l_{ba} cannot be easily determined, as for continuous longitudinal reinforcement passing through beam-column joints. The resulting expression includes, again, the axial load ratio, the mechanical transverse reinforcement ratio and the splice length-to-longitudinal bar diameter ratio, and, furthermore, the shear span-to-depth ratio, positively correlated to θ_{ult}, see **Eq. 4**. Mean, median and CoV of the observed-to-predicted ratio are 1.00, 1.00 and 0.20, see **Figure 5b**.

$$\theta_{ult} = 0.055 \cdot 0.034^{\nu} \cdot \omega_{sw}^{\ 0.15} \cdot \left(1 + 0.32 \cdot l_{ba} d_b / d\sqrt{f_c}\right) \cdot \left(0.70 + 0.30 \cdot \min\left(l_o / d_b, 50\right) / 50\right) \quad (3)$$

$$\theta_{ult} = 0.071 \cdot 0.039^{\nu} \cdot \omega_{sw}^{\ 0.18} \cdot \left(1 + 0.20 \cdot L_s / d\right) \cdot \left(0.75 + 0.25 \cdot \min\left(l_o / d_b, 50\right) / 50\right) \quad (4)$$

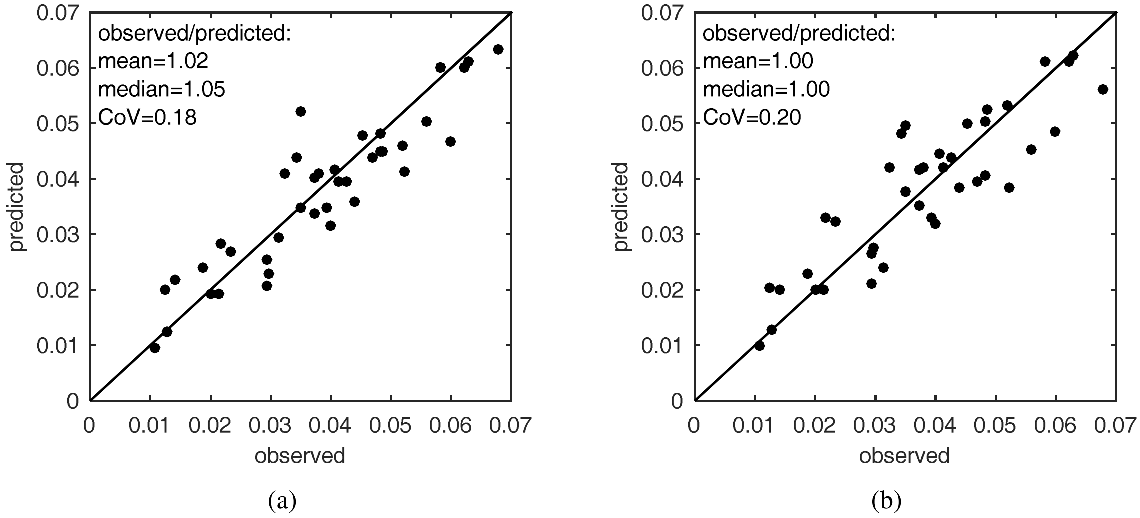

Figure 5: observed vs predicted θ_{ult} (Eq. 3 (a), Eq. 4 (b))

The obtained expressions can be compared with provisions by literature and codes for chord rotation at "ultimate". Formulations provided by the following references are considered: Eurocode 8 [18][19], without ("EC8") and with ("EC8c") correction coefficients accounting for the lack of seismic detailing and the presence of plain bars ("c.c."); Eurocode 8 with c.c. proposed by Verderame et al. [23] ("V&al"); Eurocode 8 with c.c. proposed by Melo et al. [24] ("M&al"); Biskinis and Fardis [2], without ("B&F") and with ("B&Fc"); c.c.; Zhu et al. [17], including the predicted Failure Mode ("FM_Z", "Z&al"); ASCE/SEI 41-13 [21], including the predicted Failure Mode and Condition ("FM_A", "Cond.", "ASCE"); Ghannoum [3], including the predicted Failure Mode (FM_G, G). In **Table 3**, these provisions are compared with the predictions of Eq. 3 and Eq. 4 proposed herein, and, of course, with observed values ("$\theta_{ult,obs}$"). Finally, mean, median and CoV of the observed-to-predicted ratio are reported, for all columns ("all"), and separately for columns with continuous ("c.") and lap-spliced ("l.s.") longitudinal reinforcement, too.

The Equations proposed herein show the highest predictive capacity, and similar statistics of observed-to-predicted for "c." and "l.s." columns. The comparison with uncorrected EC8 provisions highlights that only for "l.s." columns a correction should be applied; however, the c.c. proposed by code lead to a significant underestimation of deformation capacity, both for "c." and "l.s." columns. Similar trends are observed for the update proposal by Fardis and co-workers [2]. The c.c. proposed by Verderame et al. [23] and Melo et al. [24] lead to a significantly better agreement, although quite conservative for "l.s." columns in the former case, and slightly non-conservative for "c." columns and conservative for "l.s." columns in the latter case. ASCE provisions [21] appear very conservative, but a direct comparison is not possible, since these provisions are calibrated to satisfy target failure probabilities rather than to predict the expected values, and, secondarily, because the significant underestimation of the effectiveness of end-hooked anchorages of plain longitudinal bars leads to unrealistic IS and/or ID failure modes [25][47][48]. The corresponding update proposal by Ghannoum [3], aimed at predicting median deformation capacity values, is, as expected, less (but still) conservative.

#		$\theta_{ult,obs}$ [rad]	Eq. 3 [rad]	Eq.4 [rad]	EC8 [rad]	EC8c [rad]	V&al [rad]	M&al [rad]	B&F [rad]	B&Fc [rad]	FMZ*	Z&al [rad]	FMA†	Cond.	ASCE [rad]	FMG‡	G [rad]
1		0.062	0.060	0.061	0.051	0.035	0.047	0.051	0.050	0.040	F	0.037	F	ii	0.028	F-FS-S	0.040
2		0.058	0.060	0.061	0.051	0.035	0.047	0.051	0.050	0.040	F	0.037	F	ii	0.028	F-FS-S	0.040
3		0.063	0.061	0.062	0.051	0.041	0.050	0.059	0.050	0.040	F	0.037	F	ii	0.028	F-FS-S	0.040
4		0.037	0.040	0.042	0.044	0.030	0.042	0.035	0.044	0.035	F	0.029	F	ii	0.025	F-FS-S	0.034
5		0.038	0.041	0.042	0.044	0.035	0.045	0.041	0.044	0.035	F	0.029	F	ii	0.025	F-FS-S	0.034
6		0.032	0.041	0.042	0.044	0.035	0.045	0.041	0.044	0.035	F	0.029	F	ii	0.025	F-FS-S	0.034
7		0.056	0.050	0.045	0.038	0.030	0.038	0.046	0.037	0.029	F	0.026	F*	ii	0.022	F-FS-S	0.033
8		0.068	0.063	0.056	0.045	0.036	0.044	0.060	0.044	0.035	S	0.058	F*	ii	0.021	F-FS-S	0.036
9		-	-	-	0.032	0.026	0.030	0.042	0.032	0.025	F	0.044	F	ii	0.022	F-FS-S	0.033
10		0.052	0.041	0.038	0.039	0.031	0.039	0.044	0.039	0.031	S	0.040	F*	ii	0.019	F-FS-S	0.024
11		0.048	0.045	0.041	0.040	0.032	0.040	0.047	0.039	0.031	S	0.055	F*	ii	0.019	F-FS-S	0.030
12		0.019	0.024	0.023	0.038	0.030	0.039	0.022	0.037	0.030	F	-	F*	ii	0.016	F-FS-S	0.020
13		0.022	0.019	0.020	0.040	0.015	0.012	-	0.040	0.016	F	-	IS	iv	0.007	IS	0.032
14		0.013	0.020	0.021	0.040	0.020	0.021	-	0.039	0.022	F	-	F*	ii	0.017	F-FS-S	0.022
15		0.011	0.010	0.010	0.030	0.011	0.009	-	0.030	0.012	F	-	IS	iv	0.005	IS	0.030
16		0.013	0.013	0.013	0.033	0.017	0.016	-	0.032	0.018	F	-	F*	ii	0.012	F-FS-S	0.016
17		0.037	0.034	0.035	0.044	0.035	0.048	0.037	0.044	0.034	F	-	F*	ii	0.021	F-FS-S	0.027
18		0.060	0.047	0.048	0.050	0.040	0.053	0.049	0.049	0.039	F	0.006	F*	ii	0.024	F-FS-S	0.032
19		0.014	0.022	0.020	0.024	0.019	0.028	0.033	0.024	0.019	F	0.009	F*	ii	0.013	F-FS-S	0.018
20		0.035	0.052	0.050	0.052	0.035	0.044	0.048	0.051	0.040	S	0.062	F*	ii	0.022	F-FS-S	0.036
21		0.029	0.021	0.021	0.038	0.026	0.034	0.019	0.038	0.030	S	0.054	F*	ii	0.016	F-FS-S	0.023
22		0.031	0.030	0.024	0.033	0.022	0.031	0.032	0.032	0.025	S	0.054	F*	ii	0.015	F-FS-S	0.023
23		0.044	0.036	0.038	0.038	0.030	0.039	0.046	0.038	0.030	F	0.025	F*	ii	0.023	F-FS-S	0.030
24		0.047	0.044	0.040	0.040	0.032	0.040	0.051	0.039	0.031	F	0.009	ID	iv	0.004	ID	0.029
25		0.039	0.035	0.033	0.040	0.017	0.016	-	0.040	0.019	F	0.009	IS/ID	iv	0.004	IS/ID	0.029
26		0.029	0.025	0.027	0.029	0.023	0.033	0.032	0.029	0.023	F	0.011	F*	ii	0.017	F-FS-S	0.024
27		0.040	0.032	0.032	0.035	0.028	0.038	0.032	0.034	0.027	F	0.021	F*	ii	0.021	F-FS-S	0.027
28		0.020	0.019	0.020	0.024	0.019	0.027	0.027	0.024	0.019	F	0.039	F*	ii	0.017	F-FS-S	0.021
29		-	-	-	-	-	-	-	-	-	-	-	-	-	0.024	-	-
30		-	-	-	-	-	-	-	-	-	-	-	-	-	0.024	-	-
31		0.030	0.023	0.028	0.029	0.023	0.032	0.033	0.029	0.023	F	0.015	F*	ii	0.017	F-FS-S	0.026
32		-	-	-	-	-	-	-	-	-	-	-	-	-	0.024	-	-
33		-	-	-	-	-	-	-	-	-	-	-	-	-	0.024	-	-
34		0.052	0.046	0.053	0.036	0.029	0.038	0.049	0.036	0.029	F	0.030	F*	ii	0.024	F-FS-S	0.036
35		0.049	0.045	0.053	0.037	0.029	0.039	0.048	0.036	0.029	F	0.029	F*	ii	0.024	F-FS-S	0.036
36		0.034	0.044	0.048	0.047	0.038	0.049	0.053	0.046	0.037	S	0.062	F*	ii	0.022	F-FS-S	0.035
37		0.045	0.048	0.050	0.045	0.036	0.048	0.056	0.044	0.035	S	0.061	F*	ii	0.022	F-FS-S	0.035
38		0.043	0.039	0.044	0.047	0.027	0.029	-	0.046	0.029	S	0.062	IS	iv	0.007	IS	0.032
39		0.048	0.048	0.050	0.045	0.036	0.048	0.056	0.044	0.035	S	0.061	F*	ii	0.023	F-FS-S	0.035
40		0.041	0.042	0.045	0.045	0.026	0.029	-	0.045	0.028	S	0.061	IS	iv	0.009	IS	0.030
41		0.041	0.039	0.042	0.037	0.029	0.038	0.044	0.036	0.029	S	0.044	F*	ii	0.020	F-FS-S	0.031
42		0.035	0.035	0.038	0.035	0.028	0.035	0.042	0.034	0.027	S	0.034	F*	ii	0.019	F-FS-S	0.028
43		0.024	0.027	0.032	0.039	0.031	0.039	0.035	0.039	0.031	S	0.034	FS	ii	0.019	F-FS-S	0.019
44		0.022	0.028	0.033	0.038	0.030	0.038	0.038	0.038	0.030	S	0.034	FS	ii	0.019	F-FS-S	0.019
all	mean		*1.02*	*1.00*	*0.94*	*1.30*	*1.06*	*0.96*	*0.95*	*1.28*		*1.67*			*2.57*		*1.27*
	median		*1.05*	*1.00*	*0.98*	*1.35*	*1.01*	*0.94*	*0.99*	*1.31*		*1.28*			*2.02*		*1.32*
	CoV		*0.18*	*0.20*	*0.33*	*0.30*	*0.36*	*0.24*	*0.33*	*0.30*		*1.03*			*0.93*		*0.29*
c.	mean		*1.03*	*1.00*	*1.03*	*1.28*	*0.99*	*0.92*	*1.04*	*1.31*		*1.81*			*2.31*		*1.36*
	median		*1.06*	*0.99*	*1.05*	*1.31*	*1.00*	*0.92*	*1.06*	*1.34*		*1.30*			*1.93*		*1.34*
	CoV		*0.17*	*0.19*	*0.28*	*0.28*	*0.30*	*0.22*	*0.28*	*0.28*		*1.04*			*0.95*		*0.24*
l.s.	mean		*1.01*	*1.01*	*0.77*	*1.34*	*1.21*	*1.11*	*0.78*	*1.21*		*1.32*			*3.07*		*1.09*
	median		*1.04*	*1.00*	*0.84*	*1.41*	*1.19*	*1.10*	*0.85*	*1.22*		*0.69*			*2.10*		*1.29*
	CoV		*0.20*	*0.21*	*0.38*	*0.35*	*0.41*	*0.25*	*0.38*	*0.34*		*0.92*			*0.88*		*0.35*

*: F = flexure; S = flexure-shear or shear.
†: F = flexure with further confidence; F* = flexure without further confidence; FS = flexure-shear; ID: inadequate development; IS: inadequate splicing.
‡: F-FS-S = flexure or flexure-shear or shear; ID: inadequate development; IS: inadequate splicing.

Table 3: Comparison between observed and predicted chord rotation at “ultimate”

Chord rotation at zero resistance

For some tests, very high, unrealistic values of θ_0 were obtained, due to very low post-peak negative slope, unrealistically high values of θ_0 were obtained. Hence, a judgment-based value of 0.15 rad was assumed as upper bound for this parameter.

The regression obtained for θ_0 includes the axial load ratio and the geometrical transverse reinforcement ratio, see **Eq. 5**. Mean, median and CoV of the observed-to-predicted ratio, with the assumed upper bound on observed and predicted values, ratio are 0.99, 0.93 and 0.37, see **Figure 6**.

$$\theta_0 = \min\left(0.098 \cdot 0.015^{\nu} \cdot 58^{(\rho_w \cdot 100)}; 0.15\right) \tag{5}$$

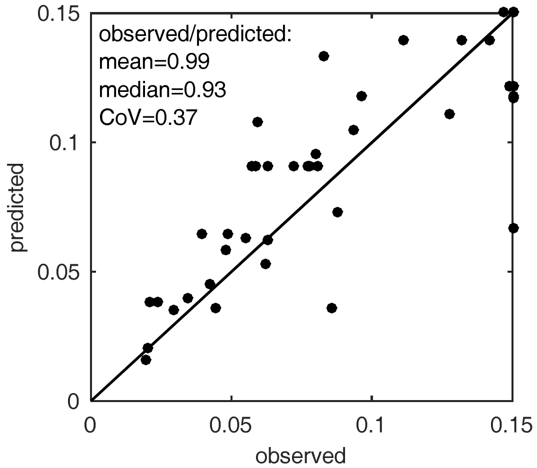

Figure 6: observed vs predicted θ_0 (Eq. 5)

<u>*Softening stiffness toward zero resistance*</u>

Due to the strict dependency between θ_0 and K_0, the adoption of a (lower) bound for this parameter is considered. To this aim, K_0 is reported versus θ_0 (see **Figure 7**): assuming a lower bound on K_0 equal to 700 kNm/rad, almost all (except two) tests with $\theta_0 \leq 0.15$ show a value of K_0 above this bound, while all the tests with $\theta_0 > 0.15$ show a value of K_0 below this bound.

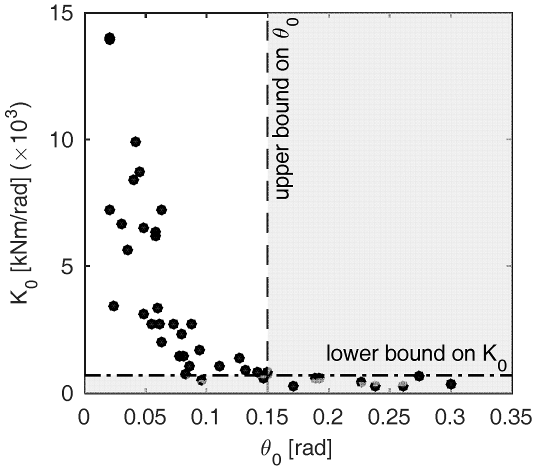

Figure 7: observed θ_0 vs observed K_0 and corresponding assumed bounds

The regression obtained for K_0 includes the same parameters of the regression obtained for θ_0, see **Eq. 6**. Mean, median and CoV of the observed-to-predicted ratio, with the assumed lower bound on observed and predicted values, ratio are 1.27, 1.00 and 0.62, see **Figure 8**.

$$K_0 = \max\left(30 \cdot 327^{\nu} \cdot \left(\rho_w \cdot 100\right)^{-1.69}; 700\right) \tag{6}$$

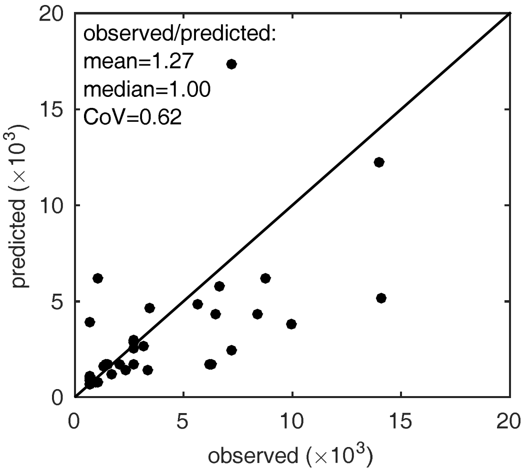

Figure 8: observed vs predicted K_0 (Eq. 6)

5 CONCLUSIONS

An empirical macro-model for the prediction of inelastic response of flexure-controlled RC columns with plain bars was proposed. To this aim, a database of cyclic tests was collected, parameters identifying the characteristic point of the response envelope were identified, and a regression analysis was performed in order to derive empirical formulations predicting these parameters. The proposed equations allow modeling the inelastic response up to complete collapse (zero-resistance condition). A comparison was carried out between proposed equations for deformability at yielding (effective stiffness) and chord rotation at "ultimate" (20% strength drop) and proposals from literature and codes, highlighting, in the latter case, a general conservatism.

The proposed formulations can be used both for performance-based deformation capacity assessment and for nonlinear modeling, thus representing a useful tool for seismic analysis of existing RC frames with plain reinforcing bars, properly accounting for the specific response characteristics of this kind of members.

6 ACKNOWLEDGEMENTS

This work was developed under the financial support of ReLUIS-DPC 2014-2018. This support is gratefully acknowledged.

REFERENCES

[1] Elwood K.J., Matamoros A.B., Wallace J.W., Lehman D.E., Heintz J.A., Mitchell A.D., Moore M.A., Valley M.T., Lowes L.N., Comartin C.D., Moehle J.P., 2007. Update to ASCE/SEI 41 concrete provisions. Earthquake Spectra, 23(3), 493-523. 1

[2] Biskinis D.E., Fardis M.N., 2010b. Flexure-controlled ultimate deformations of members with continuous or lap-spliced bars. Structural Concrete, 11(2), 93-108. 2

[3] Ghannoum W.M., 2017. Re-evaluation of modeling parameters and acceptance criteria for non-ductile and splice-deficient concrete columns. 16th World Conference on Earthquake Engineering, Santiago, Chile, January 9-13. Paper No. 1010. 3

[4] Verderame G.M., Ricci P., De Carlo G., Manfredi G., 2009a. Cyclic bond behaviour of plain bars. Part I: Experimental investigation. Construction and Building Materials, 23(12), 3499-3511.

[5] Verderame G.M., De Carlo G., Ricci P., Fabbrocino G., 2009b. Cyclic bond behaviour of plain bars. Part II: Analytical investigation. Construction and Building Materials, 23(12), 3512-3522.

[6] Verderame G.M., Fabbrocino G., Manfredi G., 2008a. Seismic response of RC columns with smooth reinforcement. Part I: Monotonic tests. Engineering Structures, 30(9), 2277-2288.

[7] Verderame G.M., Fabbrocino G., Manfredi G., 2008b. Seismic response of RC columns with smooth reinforcement. Part II: Cyclic tests. Engineering Structures, 30(9), 2289-2300. 24

[8] Haselton C.B., Liel A.B., Taylor-Lange S., Deierlein G.G., 2008. Beam-column element model calibrated for predicting flexural response leading to global collapse of RC frame buildings. PEER Report 2007/03. Pacific Earthquake Engineering Research Center, University of California, Berkeley, CA, USA. 4

[9] Ibarra L.F., Medina R.A., Krawinkler H., 2005. Hysteretic models that incorporate strength and stiffness deterioration. Earthquake Engineering and Structural Dynamics, 34(12), 1489-1511. 5

[10] Panagiotakos T.B., Fardis M.N., 2001. Deformation of reinforced concrete members at yielding and ultimate. ACI Structural Journal, 98(2), 135-148. 6

[11] Biskinis D.E., Fardis M.N., 2010a. Deformations at flexural yielding of members with continuous or lap-spliced bars. Structural Concrete, 11(3), 127-138. 7

[12] Elwood K.J., Moehle J.P., 2005a. Axial capacity model for shear-damaged columns. ACI Structural Journal, 102(4), 578-587. 8

[13] Elwood K.J., Moehle J.P., 2005b. Drift capacity of reinforced concrete columns with light transverse reinforcement. Earthquake Spectra, 21(1), 71-89. 9

[14] Elwood K.J., 2004. Modelling failures in existing reinforced concrete columns. Canadian Journal of Civil Engineering, 31(5), 846-859. 10

[15] McKenna F., Fenves G.L., Scott M.H., 2004. OpenSees: Open System for Earthquake Engineering Simulation. Pacific Earthquake Engineering Research Center. University of California, Berkeley, CA, USA. http://opensees.berkeley.edu 11

[16] Aslani H., Miranda E., 2005. Probabilistic earthquake loss estimation and loss disaggregation in buildings. Report No. 157. The John A. Blume Earthquake Engineering Center, Department of Civil and Environmental Engineering, Stanford University, Stanford, CA, USA. 12

[17] Zhu L., Elwood K.J., Haukaas T., 2007. Classification and seismic safety evaluation of existing reinforced concrete columns. ASCE Journal of Structural Engineering, 133(9), 1316-1330. 13

[18] CEN, 2005. European standard EN1998-3. Eurocode 8: Design provisions for earthquake resistance of structures. Part 3: Assessment and retrofitting of buildings. Comité Européen de Normalisation, Brussels. 14

[19] CEN, 2009. Corrigenda to EN 1998-3. Document CEN/TC250/SC8/N437A. Comité Européen de Normalisation, Brussels. 15

[20] Panagiotakos T.B., Kosmopoulos A.J., Fardis M.N., 2002. Displacement-based seismic assessment and retrofit of reinforced concrete buildings. 1st fib congress, Osaka, Japan, October 13-19. Pp. 269-278. 16

[21] ASCE, 2013. ASCE/SEI 41-13. Seismic evaluation and retrofit of existing buildings. American Society of Civil Engineers, Reston, VA, USA. 17

[22] Ghannoum W.M., Matamoros A.B., 2014. Nonlinear modeling parameters and acceptance criteria for concrete columns. ACI Special Publication, 297, 1-24. 18

[23] Verderame G.M., Ricci P., Manfredi G., Cosenza E., 2010. Ultimate chord rotation of RC columns with smooth bars: some considerations about EC8 prescriptions. Bulletin of Earthquake Engineering, 8(6), 1351-1373. 18

[24] Melo J., Varum H., Rossetto T., 2015. Experimental cyclic behaviour of RC columns with plain bars and proposal for Eurocode 8 formula improvement. Engineering Structures, 88, 22-36. 19

[25] Ricci P., Verderame G.M., Manfredi G., 2013. ASCE/SEI 41 provisions on deformation capacity of older-type reinforced concrete columns with plain bars. ASCE Journal of Structural Engineering, 139(12). 20

[26] Berry M., Parrish M., Eberhard M., 2004. PEER Structural Performance Database: User's Manual, Version 1.0. Pacific Earthquake Engineering Research Center, University of California, Berkeley, CA, USA. 21

[27] Elwood K.J., Eberhard M., 2009. Effective stiffness of reinforced concrete columns. ACI Structural Journal, 106(4), 476-484. 22

[28] Bousias S., Spathis A.L., Fardis M.N., 2007. Seismic retrofitting of columns with lap spliced smooth bars through FRP or concrete jackets. Journal of Earthquake Engineering, 11(5), 653-674. 23

[29] Di Ludovico M., Verderame G.M., Prota A., Manfredi G., Cosenza E., 2014. Cyclic behavior of nonconforming full-scale RC columns. ASCE Journal of Structural Engineering, 140(5).

[30] Di Ludovico M., 2017. Personal communication. 26

[31] Bournas D.A., Lontou P.V., Papanicolaou C.G., Triantafillou T.C., 2007. Textile-Reinforced Mortar versus Fiber-Reinforced Polymer confinement in reinforced concrete columns. ACI Structural Journal, 104(6), 740-748.

[32] Bournas D.A., Triantafillou T.C., 2009. Flexural strengthening of reinforced concrete columns with Near-Surface-Mounted FRP or stainless steel. ACI Structural Journal, 106(4), 495-505. 28

[33] Ilki A., Tezcan A., Koc V., Kumbasar N., 2004. Seismic retrofit of non-ductile rectangular reinforced concrete columns by CFRP jacketing. 13th World Conference on Earthquake Engineering, Vancouver, B.C., Canada, August 1-6. Paper No. 2236. 29

[34] Faella C., Napoli A., Realfonzo R., 2008. Cyclic flexural behavior of FRP-confined concrete columns under high axial loading. Atti del convegno ReLUIS "Valutazione e

riduzione della vulnerabilità sismica di edifici esistenti in c.a.", Rome, Italy, May 29-30. Pp. 510-520. 30

[35] Marefat M.S., Arani K.K., Hassanzadeh Shirazi S.M., Amrollahi-Biucky A., 2008. Seismic behavior and retrofit of concrete columns of old r.c. buildings reinforced with plain bars. In: Santini A., Moraci N. (editors). 2008 Seismic Engineering Conference Commemorating the 1908 Messina and Reggio Calabria Earthquake. AIP Conference Proceedings, 2008. ISBN 978-0-7354-0542-4. Volume 1020, pp. 1554-1562. doi: 10.1063/1.2963783 31

[36] Arani K.K., Marefat M.S., Amrollahi-Biucky A., Khanmohammadi M., 2010. Experimental seismic evaluation of old concrete columns reinforced by plain bars. The Structural Design of Tall and Special Buildings, 22(3), 267-290. 32

[37] Ozcan O., Binici B., Ozcebe G., 2008. Improving seismic performance of deficient reinforced concrete columns using carbon fiber-reinforced polymers. Engineering Structures, 30(6), 1632-1646.

[38] Ozcan O., 2009. Improving ductility and shear capacity of reinforced concrete columns with carbon fiber reinforced polymer. PhD Thesis. Middle East Technical University, Ankara, Turkey. 33

[39] Ozcan O., Binici B., Ozcebe G., 2010. Seismic strengthening of rectangular reinforced concrete columns using fiber reinforced polymers. Engineering Structures, 32(4), 964-973.

[40] Acun B., Sucuoglu H., 2010. Performance of reinforced concrete columns designed for flexure under severe displacement cycles. ACI Structural Journal, 107(3), 364-371. 34

[41] Acun B., Sucuoglu H., 2012a. Energy dissipation capacity of reinforced concrete columns under cyclic displacements. ACI Structural Journal, 109(4), 531-540.

[42] Acun B., Sucuoglu H., 2012b. Energy-based hysteresis model for flexural response of reinforced concrete columns. ACI Structural Journal, 109(4), 541-550.

[43] Rodriguez M., Park R., 1994. Seismic load tests of reinforced concrete columns strengthened by jacketing. ACI Structural Journal, 91(2), 150-159. 36

[44] Draper N.R., Smith H., 1998. Applied regression analysis. John Wiley & Sons, 3rd edition. 37

[45] Mander J.B., Priestley M.J.N., Park R., 1988. Theoretical stress-strain model for confined concrete. ASCE Journal of Structural Engineering, 114(8), 1804-1826. 37

[46] NZS, 2006. NZS 3101:2006. Concrete Structures Standard. Standards New Zealand, Wellington, New Zealand. 38

[47] Fabbrocino G., Verderame G.M., Manfredi G., Cosenza E., 2004. Structural models of critical regions in old-type r.c. frames with smooth rebars. Engineering Structures, 26(14), 2137-2148.

[48] Fabbrocino G., Verderame G.M., Manfredi G., 2005. Experimental behaviour of anchored smooth rebars in old type reinforced concrete buildings. Engineering Structures, 27(10), 1575-1585.